On the use of the stratified momentum balance for the deduction of shear stress in horizontal gas–liquid pipe flow

C.H. Newton *, M. Behnia

School of Mechanical and Manufacturing Engineering, University of New South Wales, Sydney 2052, Australia

Abstract

The use of the stratified flow momentum balance for the deduction of interfacial and liquid wall shear stresses from experimental measurements is examined. A systematic error analysis is applied to the governing equations using the principle of maximum uncertainty. A series of air–water experiments were conducted in 50 and 80 mm diameter pipes, in which gas pressure drop, liquid height and gas wall shear stress were measured. A framework for the correlation of the deduced shear stresses is proposed from the experimental measurements. The uncertainty analysis is used to show that the definition of mean liquid height does not significantly influence the overall results. The development of empirical equations based on such methods may lead to total uncertainties of up to 40%, irrespective of accuracy of the experimental data or the appropriateness of the correlating technique. Comparisons with state-of-the-art correlations for the liquid wall and interfacial friction factor data showed even larger discrepancies between measurement and prediction. © 1998 Elsevier Science Ltd. All rights reserved.

Keywords: Uncertainty analysis; Momentum balance; Horizontal; Two-phase; Stratified; Friction factor

1. Introduction

Despite over half a century of intensive research effort, mathematical description of gas–liquid pipe flows for engineering design calculations remains largely inadequate, due primarily to the wide variety of flow variables which must be considered. Chief amongst the parameters of interest to the pipeline designer are the mean axial pressure gradient, and the liquid holdup or void fraction. Although the advent of phenomenological or mechanistic modelling has, in the past 25 years, largely superseded several decades of development of empirical methods for the calculation of these parameters, there is a wide body of literature which suggests that even

---

* Corresponding author.

the present analytical methods may lead to large predictive errors (e.g. Spedding and Hand, 1990; Ouyang and Aziz, 1996).

Among the more common and simplest of the mechanistic models for gas–liquid pipe flow are the stratified flow momentum balance equations, proposed by Govier and Aziz (1972), and used in various forms as the basis of predictive algorithms for pressure drop and holdup calculations (e.g. Agrawal et al., 1973; Cheremisinoff & Davis, 1979; Baker et al., 1988). Taitel and Dukler (1976) were able to provide a fully generalised, compact simultaneous solution to these equations for horizontal flow, provided that significant simplifying assumptions for the definition of wall and interfacial shear stresses were used. In particular, they employed empirical correlations for the wall shear stress obtained from the smooth pipe Blasius equation for single-phase pipe flow. Although this approach has generally been found to be inadequate for two-phase flow modelling, especially in the liquid region of stratified flow (e.g. Kowalski, 1987; Ouyang and Aziz, 1996) it is still widely in use (e.g. Landman, 1991). Unfortunately, reliable generalised data correlations for both wall and interfacial shear stresses, which are able to account for the so-called diameter scaling effect, for a wide range of fluid properties and interfacial conditions, are yet to be devised, although the results of Spedding and Hand (1997) appear promising. Thus, generally speaking, accurate closure of the majority of mechanistic two-phase flow models to within the accuracies presently achievable for single-phase pipe flow is presently not possible.

Although the momentum balance equations are normally used to predict pressure gradient and liquid holdup, in this study the focus is on the estimation or deduction of wall and interfacial shear stresses from experimental measurements of these parameters in stratified gas–liquid flow. Such a technique has been used widely in rectangular ducts (e.g. Cohen and Hanratty, 1968) and has also been attempted in horizontal pipe flow by Kowalski (1987) and Andritsos and Hanratty (1987) for the purpose of developing empirical correlations for closure of the momentum equations. Although calculations of this nature are routine and can be completed without difficulty, definitive estimation of the error involved in such a process is somewhat more complex, due primarily to the non-linear relationship between the liquid height and holdup, and has not been attempted in the past. Such errors may lead to wide discrepancies in the predictions of gas–liquid flows, especially where the commonly used simultaneous solution of the phase momentum balance equations is required.

The quantification of the uncertainty in using the stratified momentum balance for the deduction of wall and interfacial shear stress from experimental measurements in air–water flows is the primary purpose of this paper. A systematic error analysis, using the principle of maximum uncertainty, is used to identify the important influences which adversely affect the accuracy in such a deduction. As a result of this analysis, the interfacial structure for wavy gas-liquid flows is examined in detail. A framework for the possible correlation of the deduced wall and interfacial shear data is also proposed.

2. The stratified momentum balance

The analysis of stratified gas–liquid pipe flow begins with the definition of the generic momentum balance in each phase for steady, one dimensional flow. In the gas region, the axial

pressure gradient $\mathrm{d}P/\mathrm{d}z$ is balanced by the gas wall and interfacial shear stresses τ_{WG} and τ_i. With reference to Fig. 1, an axial momentum balance gives:

$$PA_{\mathrm{G}} - \tau_{\mathrm{WG}}s_{\mathrm{G}}\,\mathrm{d}z - \tau_i A_i - \left(P + \frac{\mathrm{d}P}{\mathrm{d}z}\,\mathrm{d}z\right)A_{\mathrm{G}} = 0, \tag{1}$$

where A_{G} and s_{G} are the gas phase area and wall length, respectively. Commonly, the geometric terms in (1) are evaluated in terms of the average liquid height $\bar{h}_{\mathrm{L}}$, and the interfacial area, A_i, is given by:

$$A_i = s_i\,\mathrm{d}z, \tag{2}$$

where s_i is the width of the interface at $\bar{h}_{\mathrm{L}}$. It is noted that Kowalski (1987) compared calculations of the interfacial shear stress from experimental measurements using (1) with direct measurements using an extrapolation of the gas-phase Reynolds stress profile. Disagreement between the two techniques was observed to increase with interfacial wave height. Although the discrepancy was attributed to an increase in the effective interfacial area caused by the formation of surface waves, it should be noted that the results were somewhat inconclusive given the lack of either a detailed statement of experimental error, or a data set encompassing a wide range of experimental observations. Thus, for the present analysis, the conventional definition of interfacial area is tentatively retained, and substitution of (2) in (1) gives an explicit expression for the interfacial shear stress:

$$\tau_i = -\frac{1}{s_i}\left(\frac{\mathrm{d}P}{\mathrm{d}z}A_{\mathrm{G}} + \tau_{\mathrm{WG}}s_{\mathrm{G}}\right), \tag{3}$$

which can thus be used to obtain an estimation of the interfacial shear stress if the mean liquid height and gas wall shear stress are obtained experimentally. The geometric terms in (3) can be re-written in terms of the liquid height h_{L} by:
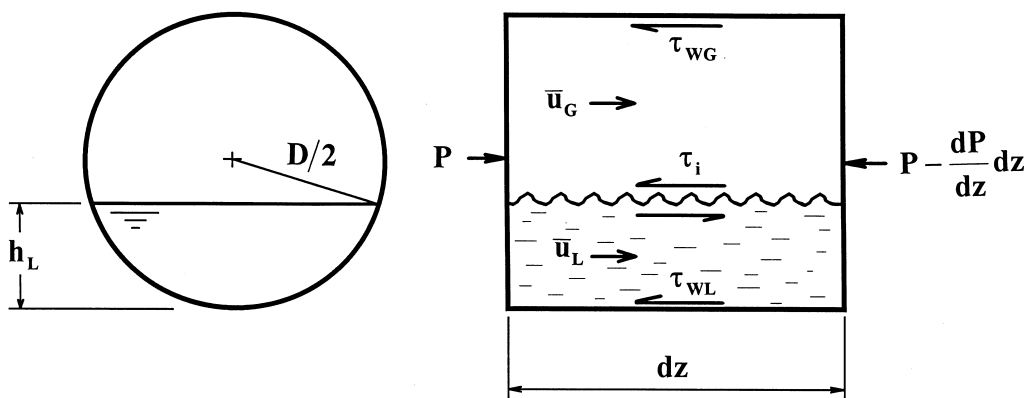

Fig. 1. Schematic description of horizontal stratified gas–liquid pipe flow.

$$s_i = 2\sqrt{h_L(D - h_L)},$$

$$s_L = D\cos^{-1}\left(1 - \frac{2h_L}{D}\right),$$

$$s_G = \pi D - s_L,$$

$$A_L = \frac{D^2}{4}\cos^{-1}\left(1 - \frac{2h_L}{D}\right) - \frac{1}{2}\sqrt{h_L(D - h_L)}(D - 2h_L),$$

$$A_G = \frac{\pi D^2}{4} - A_L, \tag{4}$$

where D is the pipe diameter, and s_L is the length of the wall wetted by the liquid. Substitution in (3) allows the interfacial shear stress to be expressed by:

$$\tau_i = -\frac{D}{2}\left[\left(\frac{D}{4}\frac{dP}{dz} + \tau_{WG}\right)\frac{\left\{\pi - \cos^{-1}\left(1 - \frac{2h_L}{D}\right)\right\}}{\sqrt{h_L(D - h_L)}} + \frac{1}{2}\frac{dP}{dz}\left(1 - \frac{2h_L}{D}\right)\right]. \tag{5}$$

A similar method can be used in the liquid region where, for a known τ_i, the liquid wall shear stress can be expressed via an axial momentum balance as:

$$\tau_{WL} = \frac{1}{s_L}\left(\tau_i s_i - \frac{dP}{dz}A_L\right). \tag{6}$$

Substitution of the relations given by (4) in (6) allows τ_{WL} to be written in terms of h_L by:

$$\tau_{WL} = \frac{\sqrt{h_L(D - h_L)}}{D\cos^{-1}\left(1 - \frac{2h_L}{D}\right)}\left[2\tau_i + \frac{D}{2}\frac{dP}{dz}\left(1 - \frac{2h_L}{D}\right)\right] - \frac{D}{4}\frac{dP}{dz}. \tag{7}$$

Provided that the average gas wall shear stress is measured, (5) and (7) can be used to evaluate the interfacial and liquid wall shear stress from experimental measurements of axial pressure gradient and liquid height, without recourse to any supplementary empirical information. Further, a knowledge of the accuracy of each individual physical measurement allows an estimation of the overall error in the deduced shear stresses, using the principle of maximum uncertainty.

3. Estimation of uncertainty in the interfacial and liquid wall shear stress

We seek to estimate how the uncertainty in the measured values of liquid height, gas wall shear stress and gas phase pressure gradient propagates into the overall uncertainty in the calculation of interfacial and liquid wall shear stress using (5) and (7). This may be done via the application of Taylors theorem, in which a function, f, of several variables can be expressed in general terms as:

$$f[(x_1 + \epsilon_1), (x_2 + \epsilon_2), \ldots, (x_n + \epsilon_n)] = f(x_1, x_2, \ldots, x_n)$$

$$+ \epsilon_1 \frac{\partial f}{\partial x_1} + \epsilon_2 \frac{\partial f}{\partial x_2} + \cdots + \epsilon_n \frac{\partial f}{\partial x_n}$$

$$+ \frac{\epsilon_1^2}{2} \frac{\partial^2 f}{\partial x_1^2} + \frac{\epsilon_2^2}{2} \frac{\partial^2 f}{\partial x_2^2} + \cdots + \frac{\epsilon_n^2}{2} \frac{\partial^2 f}{\partial x_n^2} + \cdots \text{ etc.,} \qquad (8)$$

where x_n represents n variables, and ϵ_n the uncertainty in each of these variables. Neglecting the higher order terms, and using absolute values (since it is assumed that the probability of positive and negative uncertainties is equal), (8) can be re-written in terms of the overall uncertainty in f, ϵ_f, as:

$$\epsilon_f = f[(|x_1| + |\epsilon_1|), (|x_2| + |\epsilon_2|), \ldots, (|x_n| + |\epsilon_n|)] - f(|x_1|, |x_2|, \ldots, |x_n|)$$

$$= \left| \epsilon_1 \frac{\partial f}{\partial x_1} \right| + \left| \epsilon_2 \frac{\partial f}{\partial x_2} \right| + \cdots + \left| \epsilon_n \frac{\partial f}{\partial x_n} \right|. \qquad (9)$$

With reference to (5), the maximum uncertainty in the calculation of τ_i is obtained by using (9):

$$\epsilon_{\tau_i} = \frac{\partial \tau_i}{\partial h} \epsilon_h + \frac{\partial \tau_i}{\partial \left(\frac{dP}{dz} \right)} \epsilon_{dP/dz} + \frac{\partial \tau_i}{\partial \tau_{WG}} \epsilon_{\tau_{WG}}, \qquad (10)$$

where it is assumed that D is known with certainty, and where ϵ_h, $\epsilon_{dP/dz}$ and $\epsilon_{\tau_{WG}}$ represent the uncertainty in the measured values of liquid height, axial pressure gradient and gas wall shear stress, respectively.

The partial derivatives in (10) are expressed by:

$$\frac{\partial \tau_i}{\partial h} = \frac{1}{2} \left[\frac{dP}{dz} + \frac{2}{s_i} \left(\frac{D}{4} \frac{dP}{dz} + \tau_{WG} \right) \left\{ \frac{2 s_G D}{s_i^2} \left(1 - \frac{2 h_L}{D} \right) + \frac{1}{\gamma} \right\} \right],$$

$$\frac{\partial \tau_i}{\partial \left(\frac{dP}{dz} \right)} = -\frac{A_G}{s_i},$$

$$\frac{\partial \tau_i}{\partial \tau_{WG}} = -\frac{s_G}{s_i}, \qquad (11)$$

where

$$\gamma = \sqrt{\frac{h_L}{D} \left(1 - \frac{h_L}{D} \right)}.$$

Similarly, the maximum uncertainty in τ_{WL}, evaluated from (7) can be expressed as

$$\epsilon_{\tau_{WL}} = \frac{\partial \tau_{WL}}{\partial h} \epsilon_h + \frac{\partial \tau_{WL}}{\partial \left(\frac{dP}{dz} \right)} \epsilon_{dP/dz} + \frac{\partial \tau_{WL}}{\partial \tau_i} \epsilon_{\tau_i}, \qquad (12)$$

where the partial derivatives are given by:

$$\frac{\partial \tau_{WL}}{\partial h} = \frac{1}{s_L}\left[2\tau_i + \frac{D}{2}\frac{dP}{dz}\left(1 - \frac{2h_L}{D}\right)\right]\left[\frac{(D - 2h_L)}{s_i} - \frac{2_i}{2\gamma s_L}\right] - \frac{s_i}{2s_L}\frac{dP}{dz},$$

$$\frac{\partial \tau_{WL}}{\partial\left(\frac{dP}{dz}\right)} = -\frac{A_L}{s_L},$$

$$\frac{\partial \tau_{WL}}{\partial \tau_i} = \frac{s_i}{s_L}. \tag{13}$$

4. Experimental data

Two long, horizontal flowlines, constructed from 50 and 80 mm internal diameter smooth acrylic pipes, were used to record axial pressure drop, liquid height, and gas wall shear stress data in stratified air–water flow. The entrance length to each measurement station was 10.4 m, giving entrance length-to-diameter ratios of 208 and 130 for the 50 and 80 mm pipes, respectively. It is noted that Massey (1989) has recommended an entrance length of 125 pipe diameters to ensure fully developed flow. To check for this flow condition in the present experiments, the presence of a steady streamwise pressure gradient was verified by measuring the static pressure at various axial locations. It is also noted that stratified flow is characterised by small axial pressure gradients, precluding significant effects due to gas expansion. Further, no interface level gradients were observed in the liquid, suggesting that the entrance lengths were sufficient to obtain fully developed flow at the measurement stations. A complete description of the experimental apparatus used is given in Newton and Behnia (1996), and is not repeated here.

Measurements of the instantaneous liquid height at the centre of each pipe were obtained using a wire conductance probe. This device was similar in concept to that described by Brown et al. (1978), but designed to provide a linear relationship between the output voltage and the liquid height, over the range of liquid heights encountered during the experiments. This relationship was verified experimentally. The probe itself consisted of a pair of 0.2 mm diameter stainless steel wires mounted vertically in the pipe, and spaced 1.5 mm apart. Both the oscillator frequency and wire spacing were varied to assess their effect on the results, but none was found. The output from the probe was interfaced with a computer data acquisition system which allowed sampling and averaging of the instantaneous liquid height measurements for the calculation of the mean liquid height and the RMS wave height, and for the storage of the time-dependant instantaneous height profiles. Typically, the liquid height was sampled for 10 s at 200 Hz, which was a rate approximately an order of magnitude greater than the highest frequency interfacial disturbance.

Testing was conducted by varying the gas velocity at fixed liquid flow rates. When the gas velocity was set, sufficient time was allowed for the flow to settle, and the axial pressure drop, and liquid and gas flow rates, were measured. The time dependent instantaneous liquid height was recorded by the computer for a set sampling rate and time. A Preston tube, used for

measurement of the gas wall shear stress, was then traversed around the pipe wall from the top of the pipe to a position just above the gas–liquid interface, such that the probe remained clear of the wave crests, and then back again. The pressure drop, flow rates, and the liquid height were then re-measured to ensure that the flow conditions had remained stable. At the conclusion of each experiment the gas velocity was increased and the process repeated. The experiments encompassed smooth, rippled, and wavy interfacial conditions.

5. Results and discussion

5.1. Characterisation of the interface

The characterisation of two-phase flows is a somewhat subjective process, even within the stratified flow regime. In the present study, the nature of observed interfacial disturbances was classified into three broad categories for convenience, although it is noted that several other more complex descriptions of such flows have appeared in the literature (e.g. Cohen and Hanratty, 1968; Spedding and Hand, 1990). The present flow regimes are described as follows:

1. Smooth. The interface was completely flat and no disturbance was visible. Such a flow generally occurs at relatively low gas flow rates.
2. Rippled. The interface contained small amplitude, small wavelength disturbances which were distributed relatively evenly across and along its surface. This flow occurs at relatively low liquid and high gas flow rates, with a likely transition to film or annular flow with a large increase in the gas velocity.
3. Wavy. The interface contained large amplitude and large wavelength disturbances which propagated axially along the liquid surface in either a steady or an unsteady manner. For those waves which travelled with constant velocity, the cross stream variation in wave height was almost negligible and the disturbance may be considered to be two-dimensional. Where unsteady surface ('roll') waves existed the wave front was almost always observed to break from the centre of the interface towards the walls. This type of flow occurs at high gas and liquid flow rates, and is usually the precursor to a transition to slug flow. In general, such waveforms induce substantial interfacial curvature, and are thus not suitable for inclusion in the present analysis.

Typical profiles of the time dependant liquid height measured at the centre of the interface by the conductance probes are shown in Fig. 2. The flow is interpreted as being from right to left. For the rippled flow shown in this figure, the wave amplitude was in the order of 1 mm and the period 0.05 s, and these characteristics were approximately representative of all the rippled flows observed, irrespective of the pipe diameter. Fig. 2(b) and (c) compare the form of larger two-dimensional waves in the 50 and 80 mm diameter pipes, respectively, where the two flows had approximately similar phase velocities and liquid holdups. The resemblance in amplitude, period and shape between the waveforms is quite striking, suggesting that it is the dynamics of the flow (i.e. the relative momentum of the two phases) that determines the structure of the interface, and not the pipe diameter. It is also interesting to note that an increase in the
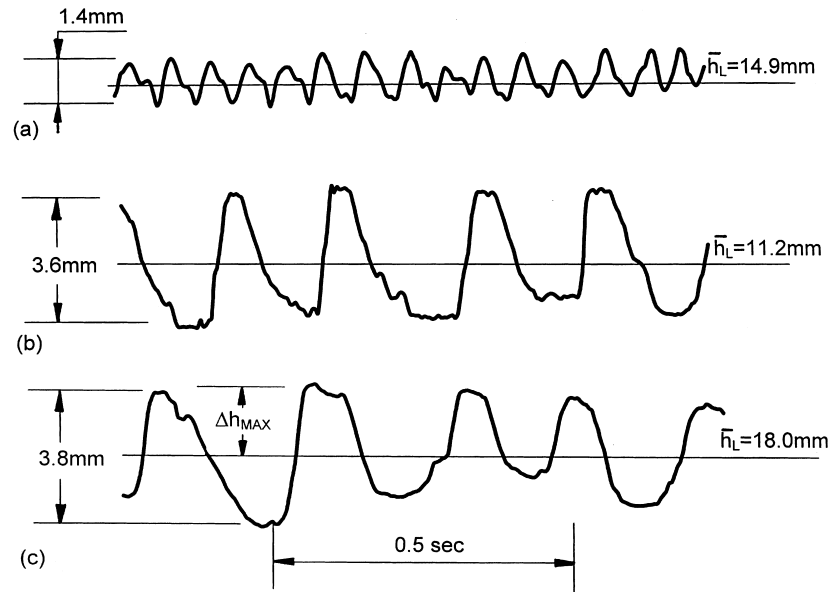
Fig. 2. Instantaneous centreline liquid height profiles: (a) $u_L = 0.12$ m/s, $u_G = 4.1$ m/s, $H_L = 0.250$, $D = 50$ mm, (b) $u_L = 0.30$ m/s, $u_G = 6.6$ m/s, $H_L = 0.167$, $D = 50$ mm, (c) $u_L = 0.30$ m/s, $u_G = 5.6$ m/s, $H_L = 0.168$, $D = 80$ mm. Note the near dynamic similarity of cases (b) and (c), reflected in the similar interfacial structure, despite the difference in pipe diameter.

relative velocity of the phases led to significant changes in the wave period, but not in the wave height. These observations form the basis of the scaling effect in two-phase pipe flows. The size of interfacial disturbances for flows with similar relative velocities is approximately equal, and an increase in the pipe diameter merely serves to decrease the relative roughness of the interface itself, with a consequent non-linear effect on the momentum balance between the gas and the liquid. As may be seen in Table 1, for the ranges of flows considered, the range of interfacial disturbances was approximately the same for both pipe sizes.

For a mathematical description of the interface, the wave height Δh_{MAX}, defined in Fig. 2, was estimated by visual inspection of the time dependent liquid height profiles for each data point. The results obtained from this analysis are shown in Table 1. The root-mean-square (RMS) wave height is calculated from

$$\Delta h_{RMS} = \sqrt{\frac{\sum_{i=1}^{n}(h_{Li} - \bar{h}_L)^2}{n}} \tag{14}$$

where h_{Li} is the time dependent instantaneous liquid height, n is the number of samples, and $\bar{h}_L$ is the mean liquid height, given by:

$$\bar{h}_L = \frac{\sum_{i=1}^{n} h_{Li}}{n}. \tag{15}$$

The relationship between the RMS and maximum wave heights is shown in Fig. 3, where it can be seen that the maximum wave size in the experiments reported here was approximately

Table 1
Description of measured data

	$\bar{u}_L$ (m/s)	$\bar{u}_G$ (m/s)	$\bar{h}_L$ (mm)	Δh_{MAX} (mm)	Δh_{RMS} (mm)	dP/dz (Pa/m)
$D = 50$ mm	0.12	4.1	14.9	0.7	0.53	8.0
	0.12	4.8	14.8	0.8	0.50	10.6
	0.17	5.2	11.5	0.9	0.47	14.2
	0.20	6.4	10.2	0.9	0.46	21.2
	0.24	7.1	9.2	1.1	0.56	26.0
	0.17	3.4	21.3	1.0	0.60	7.1
	0.18	4.0	20.2	2.6	1.56	11.4
	0.20	4.5	18.8	2.7	1.45	15.3
	0.21	5.0	18.1	2.7	1.63	18.5
	0.23	5.5	17.0	3.1	1.58	19.7
	0.14	3.1	19.7	0.3	0.18	4.5
	0.14	3.8	19.5	0.7	0.46	6.4
	0.15	4.4	18.3	1.2	0.73	9.2
	0.17	5.0	16.8	2.3	1.35	13.8
	0.19	6.0	15.3	2.1	1.13	19.7
	0.3	6.6	11.2	1.8	0.94	23.0
$D = 80$ mm	0.26	4.6	20.3	1.8	0.94	6.6
	0.28	5.2	18.9	2.0	1.01	8.1
	0.30	5.6	18.0	1.9	0.97	8.7
	0.23	4.7	18.2	1.7	0.87	5.9
	0.29	5.8	15.6	1.4	0.70	8.3
	0.27	4.3	24.6	3.0	1.48	6.6
	0.34	5.0	21.0	2.6	1.13	8.8
	0.40	6.2	18.8	2.8	1.42	10.8
	0.20	3.9	20.5	1.0	0.59	3.9

4 mm. Irrespective of the interfacial disturbance encountered, a strong linear relationship exists between these parameters, which is given by:

$$\Delta h_{RMS} \approx 0.53 \Delta h_{MAX}. \tag{16}$$

For air–water stratified flow in a horizontal channel, Cohen and Hanratty (1968) have observed the constant in (16) to be closer to 0.47. Paras and Karabelas (1991) obtained a value of 0.35 for horizontal annular air-water pipe flow. It is interesting to note that a standard sine wave, which is commonly used in analytical models of interfacial wave motion (e.g. Buckles et al., 1984), incorporates a uniform shape on the windward and leeward sides, and has a proportionality constant of 0.707. Clearly, the present results indicate that neither the symmetry nor the shape of the standard sine wave adequately represents surface waves in stratified gas–liquid flows.

5.2. Estimation of maximum uncertainty in the deduced shear stresses

The experimental data was used to calculate the interfacial and liquid wall shear stresses using (3) and (6). For the estimation of uncertainty in these calculations, a reasonable estimate
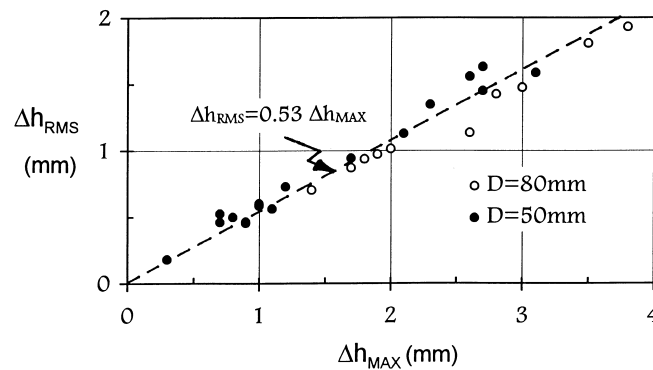
Fig. 3. Relationship between the RMS and maximum wave height for both pipe diameters.

of the experimental errors is required. For the interfacial shear stress, the parameters of interest are the axial pressure gradient (which is assumed to be equal in the liquid and gas phases), the gas wall shear stress, and the liquid height. In the case of the liquid wall shear stress, estimation of the uncertainty in the axial pressure gradient, liquid height, and interfacial shear stress is required.

The uncertainty in the axial pressure gradient is obtained from the accuracy of the Betz manometer, which has a resolution of 0.05 mm H_2O (=0.49 Pa). Given that the test section pressure gradient is measured over 2 m, then $\epsilon_{dP/dz} = 0.25$ Pa/m over the entire range of data.

The uncertainty in the gas wall shear stress is obtained from the calibration of the Preston tube in a single phase pipe flow, and from comparison with other published correlations as described in Newton and Behnia (1996). For the purposes of this analysis, it is conservatively estimated that $\epsilon_{\tau_{WC}} = 0.05\tau_{WG}$ for all the data.

Estimation of the uncertainty in the liquid height is not so straightforward because of the time dependant nature of the interface. Since the relationship between the liquid height and the liquid holdup is clearly non-linear for pipe flow, this parameter is potentially quite significant to the overall results. The conductance probe was calibrated regularly and can be considered to be accurate to within 1% of a static, smooth liquid height, and any appreciable uncertainty in this parameter must come from a consideration of the relationship between the time averaged mean value and the wave height. Since it has been postulated that the effective mean liquid height for gas–liquid flows with a wavy interface may be different from the time averaged value as a result of sheltering (Kordyban, 1974), a further source of uncertainty in this parameter therefore arises. As a basis for estimation of the maximum uncertainty, one is then left with a choice between the maximum and the RMS wave height. If the effective mean liquid height is displaced from the time averaged value, it is unlikely that such a displacement will be greater than the RMS wave height, which is therefore chosen for the analysis.

The maximum uncertainty in the interfacial shear stress calculations, obtained from (10), is shown in Fig. 4. The effect of the uncertainty in liquid height can also be seen in the figure. Given that from (16) the RMS wave height is approximately 53% of the maximum wave height, the effect of using the latter in the uncertainty calculations may be readily deduced from the figure.
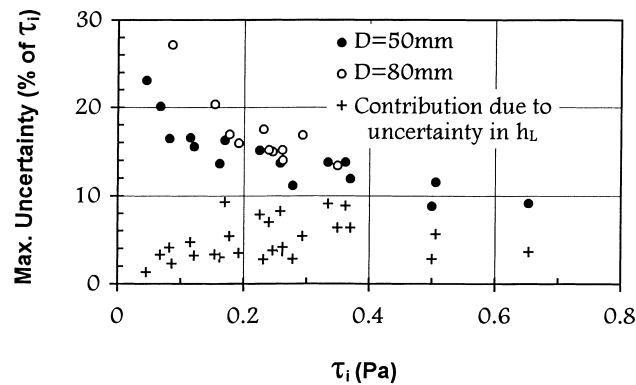
Fig. 4. Distribution of maximum uncertainty in the interfacial shear stress calculations.

Generally speaking, the maximum uncertainty in the interfacial shear stress peaked at approximately 20–25% of the calculated value at the lower flow rates and approached a value lower than 10% as the flow rate increased. The uncertainty was slightly higher in the 80 mm pipe calculations. Surprisingly, as the relative phase flow rates and therefore the shear stress is decreased, it is the errors in the measurement of the pressure gradient which become dominant, despite the accurate resolution of the manometer, and relatively large wave height to mean liquid height ratios. The effect becomes more significant in the 80 mm diameter pipe where the axial pressure gradients are lower. The uncertainty in the liquid height became more important as the shear stress was increased, but even under these circumstances it rarely contributed to more than 50% of the overall uncertainty. The error in the gas wall shear stress measurements was generally the least dominant term. Evidently the definition of mean liquid height may not be as significant to the integrity of the stratified momentum balance as previously thought. Further, the magnitude of the uncertainty may account for the aforementioned inconsistencies in the results of Kowalski (1987).

The results for the liquid wall shear are shown in Fig. 5, where it is observed that the maximum uncertainty is generally in the order of 8–15% except at the lowest shear stress values. In this instance, the maximum uncertainty is comprised almost exclusively of the uncertainty in the interfacial shear stress. There is almost no direct influence of the liquid height or the pressure gradient on the overall result, although it is noted that these factors do have an indirect influence via the uncertainty in the interfacial shear.

Finally, it is noted that Ouyang and Aziz (1996) have evaluated the momentum balance equations using a simplified error analysis and observed that it is the correlations used for liquid and gas wall shear, and not the experimental accuracy, that is primarily responsible for inaccuracies in calculations of the interfacial shear stress using (3) and (6). The present experiments were carefully controlled to ensure that the experimental uncertainty in each of the measured variables could be accurately estimated. From our results we can only conclude that the use of (1) and (3) in conjunction with even the most accurate experimental data will yield appreciable uncertainty in the calculation of interfacial and liquid wall shear stress. This uncertainty should be accounted for when using correlations based on the measured data, especially in iterative solutions of (1) and (3) for pressure gradient and holdup.
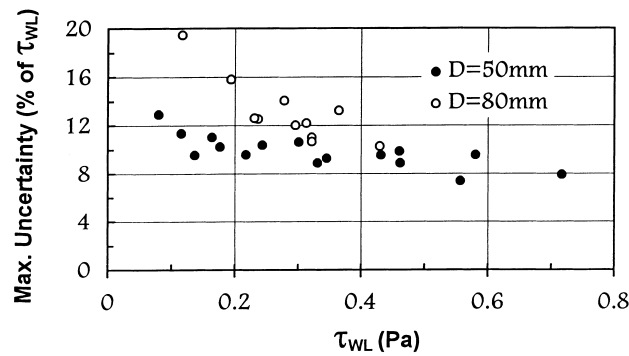
Fig. 5. Distribution of maximum uncertainty in the liquid wall shear stress calculations.

5.3. Correlation of liquid wall and interfacial shear stress

The interfacial friction factor is obtained from the experimental measurements using:

$$f_1 = \frac{2\tau_i}{\rho_G (\bar{u}_G - \bar{u}_L)^2} \tag{17}$$

where $\bar{u}_L$ and $\bar{u}_G$ are the liquid and gas velocities, averaged over the mean phase cross sectional area, and ρ_G is the gas density. The liquid wall friction factor is obtained in a similar manner, and is defined by:

$$f_L = \frac{2\tau_{WL}}{\rho_L \bar{u}_L^2} \tag{18}$$

where ρ_L is the liquid density.

Andritsos and Hanratty (1987), Kowalski (1987), and Spedding and Hand (1990) have proposed equations for interfacial friction factor based on experimental and analytical methods in horizontal gas–liquid pipe flows, similar to those used here. More recently, Ouyang and Aziz (1996) have used a comprehensive data bank to develop correlations for liquid wall and interfacial friction factors over a wide range of fluid properties and pipe diameters. However, in none of these papers was a systematic error analysis of the results performed. Further, the majority of these correlations are limited to air–water flow, for a specific type of interfacial disturbance, and are likely to be diameter dependant.

In this study a basis for correlating the measured interfacial friction data arises from a consideration of the analysis of uncertainty. Kowalski (1987) used the results of Pimsner and Toma (1977) to suggest the following basic functional relationship:

$$f_i = f(H_L, Re_G, Re_L) \tag{19}$$

where H_L is the liquid holdup, and Re_G and Re_L are the phase gas and liquid Reynolds numbers, respectively. In the present study, the Reynolds numbers are obtained using the phase hydraulic diameters although Kowalski (1987) used the pipe diameter, and obtained a reasonable correlation of data obtained in a 50 mm pipe.
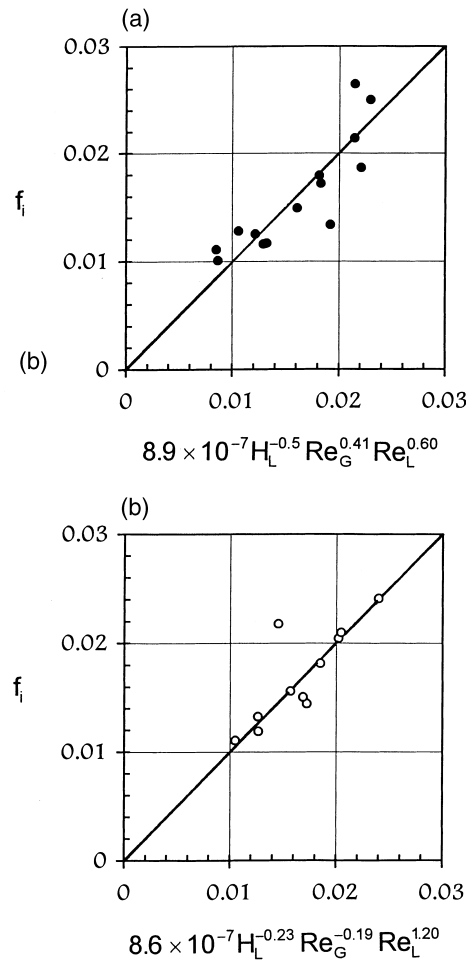
Fig. 6. Comparison of correlating function for interfacial shear stress with measured values (a) $D = 50$ mm, (b) $D = 80$ mm.

The form of (19) is representative of the aforementioned observations regarding the nature of the interface. The dynamics of each phase is represented by its Reynolds number, and the width or geometry of the interface relative to the wetted perimeter in each phase is accounted for by the liquid holdup. The effect of pipe scaling, required to account for the non-linear relationship between wave height and pipe diameter, may lead to a diameter dependence in the correlating constants.

Eq. (19) was applied to the experimental data obtained in each pipe separately, and the results are shown in Fig. 6. The agreement between the derived equations and the experimental data appears to be quite satisfactory, which is encouraging because the entire range of interfacial conditions are incorporated in the results. A comparison of the correlating constants in each equation shows that they are of the same order of magnitude, which suggests a possible influence of pipe diameter. However, more extensive data sets incorporating a wider range of pipe diameters is required to draw more definite conclusions.
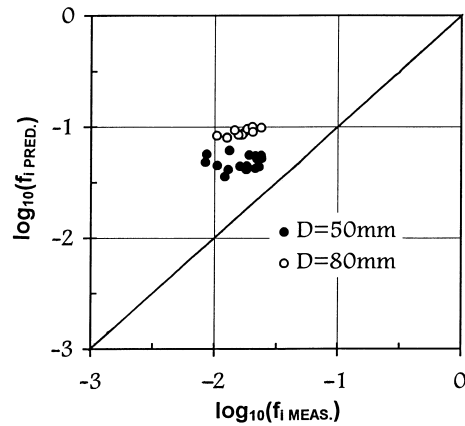
Fig. 7. Comparison of the measured interfacial friction factor data with the correlation of Ouyang and Aziz (1996).

The measured interfacial shear data are compared with the recent correlation of Ouyang and Aziz (1996) in Fig. 7. The data are plotted in logarithmic form, for ease of comparison with the results in their paper. A diameter dependence is clearly observed, with predictions for the larger pipe up to an order of magnitude greater than the measured values. It is noted that there is a substantial difference between the data and their correlation. Nonetheless, the present measurements fall within the range of the data reported in their paper. Evidently, the form of the equations presented by Ouyang and Aziz is not entirely successful in removing the effects of variable pipe diameter and fluid properties, even within the stratified flow regime, despite the large database on which it is founded.

The measured liquid wall friction factors are compared with the commonly used single phase pipe flow Blasius equation in Fig. 8, where the agreement is observed to be quite poor. This
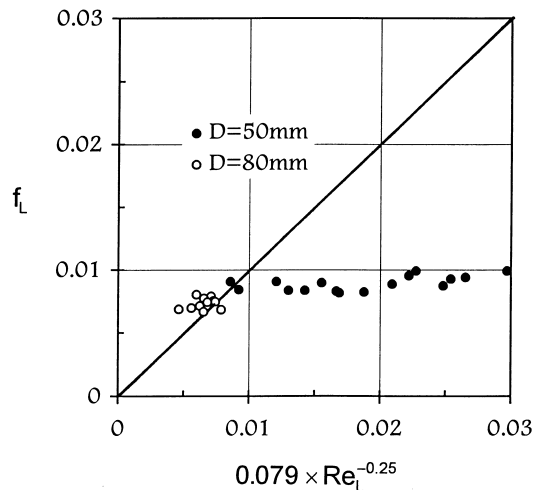

Fig. 8. Comparison of the measured liquid wall friction factors with the Blasius equation for smooth wall single phase pipe flow.

result has also been observed by Kowalski (1987) and Ouyang and Aziz (1996). One might expect that the liquid wall friction factor for each pipe diameter will be well correlated by a function of the form:

$$f_L = f(H_L, Re_L) \tag{20}$$

or even by (19), but the present attempts to obtain accurate correlations using these functions were unsuccessful. It should be noted that Ouyang and Aziz (1996) have proposed a relationship quite similar to (20), based on a large number of data points. Their correlation for liquid wall friction factor is shown in Fig. 9, where it can be seen that the predictions overpredict the measured values, sometimes by as much as 200%.

Consideration of (6) reveals that the liquid flow is dominated by the interfacial shear stress, especially at low liquid holdups, with the axial pressure gradient having considerably less influence because of the reduced liquid cross section. This is why expressions developed for full pipe flow are simply not applicable to the liquid region. Under such circumstances, it might be expected that a strong relationship exists between the interfacial and liquid wall friction factors. Such a relationship is shown in Fig. 10, where agreement is excellent for data from both pipe diameters.

Finally, on the basis of the data correlations developed here, it is possible to estimate the overall uncertainty in their use. The maximum uncertainty derived from the calculation of the shear stress ϵ_C, may be combined with the estimated maximum uncertainty in the correlating functions ϵ_F, by:

$$\epsilon_{TOT} = \sqrt{\epsilon_C^2 + \epsilon_F^2}. \tag{21}$$

From Fig. 6(a) it is estimated that the maximum uncertainty in the data correlation for f_i in the 50 mm diameter pipe is 30%, and a conservative estimate for the maximum uncertainty in the calculation procedure is 20%, giving an overall uncertainty in the final equation of 36%. These calculations are summarised in Table 2. On the basis of these results it can be observed that even for a well controlled experimental setup, and a data correlating function tailored
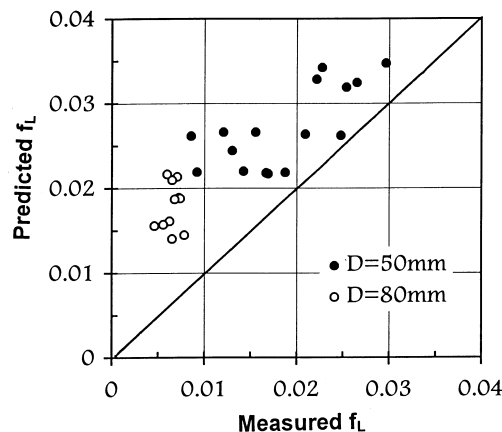

Fig. 9. Comparison of the measured liquid wall friction factor data with the correlation of Ouyang and Aziz (1996).
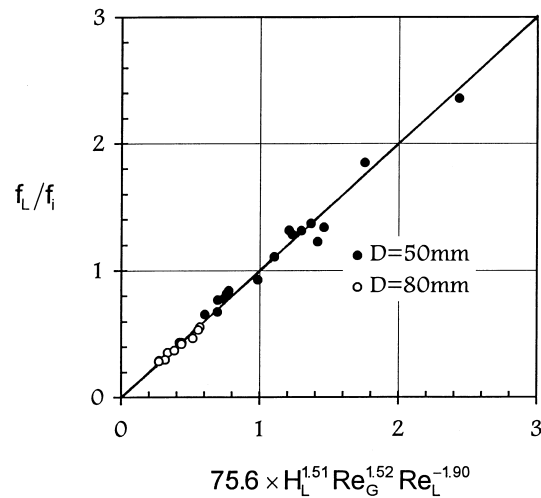
Fig. 10. Proposed form of correlation for liquid wall friction factor

specifically to the results obtained by consideration of the stratified momentum balance equations, one is still compelled to accept a maximum uncertainty of up to almost 40% in the prediction of interfacial and liquid wall shear stresses for horizontal gas–liquid pipe flows.

6. Conclusions

A systematic analysis of uncertainty combined with a series of experimental results has been used to evaluate the use of the stratified flow momentum balance for the deduction of interfacial and liquid wall shear stress in horizontal gas–liquid pipe flow. A framework for correlating the calculated values has been proposed, and its effect on the overall uncertainty of the results evaluated.

It was observed that uncertainty in the definition of mean liquid height does not have a significant effect on the performance of the momentum balance equations, even at low liquid holdups. For flows characterised by small shear stress values, the inaccuracy in the measurement of the axial pressure gradient is the dominant source of uncertainty. For the experimental data reported here, the maximum uncertainty in the interfacial shear stress

Table 2
Estimation of the overall uncertainty in the development of correlations for interfacial and liquid wall friction factor

	f_i			f_{WL}		
	ϵ_C (%)	ϵ_F (%)	ϵ_{TOT} (%)	ϵ_C (%)	ϵ_F (%)	ϵ_{TOT} (%)
$D = 50$ mm	20	30	36	11	15	19
$D = 80$ mm	22	25	33	13	15	20

calculations decreased and approached 10% as the flow rates of the phases were increased. The maximum uncertainty in the calculation of liquid wall shear stress followed a similar trend, and appeared to approach a value of approximately 8% at sufficiently high flow rates.

It is noted that empirical equations based on the use of the shear stress data obtained using from the use of the stratified flow momentum balance equations may have total uncertainties of up to 40%, irrespective of how stringently the uncertainty in each of the experimental parameters is controlled. When the measurements were compared with state-of-the-art data correlations, the discrepancy was observed to be even higher. The effect of uncertainty in the liquid wall and interfacial shear stress on the iterative solution of the stratified momentum balance equations for pressure drop and liquid holdup is still to be ascertained.

References

Agrawal, S.S., Gregory, G.A., Govier, G.W., 1973. An analysis of horizontal stratified two-phase flow in pipes. Canadian Journal of Chemical Engineering 51, 280–286.

Andritsos, N., Hanratty, T.J., 1987. Influence of interfacial waves in stratified gas–liquid flows. AIChE Journal 33, 444–454.

Baker, A., Nielsen, K., Gabb, A., 1988. Pressure loss, liquid holdup calculations developed. Oil and Gas Journal , 55–59.

Brown, R.C., Andreussi, P., Zanelli, S., 1978. The use of wire probes for the measurement of liquid film thickness in annular gas liquid flows. Canadian Journal of Chemical Engineering 56, 754–757.

Buckles, J., Hanratty, T.J., Adrian, R.J., 1984. Turbulent flow over large-amplitude wavy surfaces. Journal of Fluid Mechanics 140, 27–44.

Cheremisinoff, N.P., Davis, E.J., 1979. Stratified turbulent-turbulent gas–liquid flow. AIChE Journal 25, 48–56.

Cohen, L.S., Hanratty, T.J., 1968. Effect of waves at a gas–liquid interface on a turbulent air flow. Journal of Fluid Mechanics 31, 467–479.

Govier, G.W., Aziz, K., 1972. The Flow of Complex Mixtures in Pipes. van Nostrand Reinhold, New York.

Kordyban, E., 1974. Interfacial shear in two-phase wavy flow in closed horizontal channels. ASME Journal of Fluids Engineering 96, 97–102.

Kowalski, J.E., 1987. Wall and interfacial shear stress in stratified flow in a horizontal pipe. AIChE Journal 33, 274–281.

Landman, M.J., 1991. Non-unique holdup and pressure drop in two-phase stratified inclined pipe flow. International Journal of Multiphase Flow 17, 377–394.

Massey, B.S., 1989. Mechanics of Fluids. van Nostrand Reinhold, London.

Newton, C.H., Behnia, M., 1996. Estimation of gas wall shear stress in horizontal stratified gas–liquid pipe flow. AIChE Journal 42, 2369–2373.

Ouyang, L-B., Aziz, K., 1996. Development of new wall friction factor and interfacial friction factor correlations for gas–liquid stratified flow in wells and pipelines. In: Paper SPE35679, Proc. SPE Western Regional Meeting, Anchorage, Alaska, pp. 285–295.

Paras, S.V., Karabelas, A.J., 1991. Properties of the liquid layer in horizontal annular flow. International Journal of Multiphase Flow 17, 439–454.

Pimsner, V., Toma, P., 1977. The wavy aspect of a horizontal co-current air-water film flow and the transport phenomena. International Journal of Multiphase Flow 3, 273–283.

Spedding, P.L., Hand, N.P., 1990. Prediction of holdup and pressure loss from the two-phase momentum balance for stratified type flows. In: Proc. ASME-FED Advances in Gas–liquid Flows. Dallas, Texas, pp. 73–87.

Spedding, P.L., Hand, N.P., 1997. Prediction in stratified gas–liquid co-current flow in horizontal pipelines. International Journal of Heat and Mass Transfer 40, 1923–1935.

Taitel, Y., Dukler, A.E., 1976. A model for predicting flow regime transitions in horizontal and near horizontal gas–liquid flow. AIChE Journal 22, 47–55.